ELSEVIER

Catalysis Today 49 (1999) 431–440

CATALYSIS TODAY

Molybdenum catalyzed ethylene carbonylation. II. Spectroscopic investigation of the reactions and equilibria of molybdenum hexacarbonyl and molybdenum halocarbonyls under reaction conditions

Joseph R. Zoeller*, Norma L. Buchanan, Todd J. Dickson, Kristine K. Ramming

Eastman Chemical Company Research Laboratories, PO Box 1972, Kingsport, TN 37662-5150, USA

Abstract

A surprisingly efficient carbonylation of ethylene to yield propionic anhydride and propionic acid using halide promoted $Mo(CO)_6$ catalysts has been recently reported in the literature. Although the earlier report included detailed kinetics and a unique mechanistic interpretation involving a metalloradical process, the spectroscopic examination, which played an important role in clarifying the reaction mechanism, was only described qualitatively. This report describes the in situ infrared spectroscopic investigation of the chemistry of the molybdenum carbonyl catalysts in greater detail. Emphasis will be on the spectroscopic examinations of the equilibria of $Mo(CO)_6$ and the molybdenum halocarbonyls, the oxidation of Mo(0) with alkyl halides, and in situ regeneration of the active catalyst under reaction conditions. As part of this investigation, a general method for the determination of equilibrium constants for reactions involving infrared active species using attenuated total reflectance technique, ATR, is described wherein neither the extinction coefficient nor the effective pathlength are known with certainty. The method is demonstrated using the equilibrium between $Mo(CO)_6$ and $Mo(CO)_5I^-$ as an example.

Keywords: Carbonylation; Molybdenum; Ethylene; Carbon monoxide

1. Introduction

Our group has recently described a surprisingly efficient carbonylation of ethylene to generate propionate derivatives, such as propionic anhydride, propionic acid, and methyl propionate according to reaction (1) [1]. The key requirements for this reaction were molybdenum hexacarbonyl, an alkyl halide (generally added as the ethyl halide), a halide salt (or salt precursor), and of course, the reactants, ethylene and carbon monoxide. In addition, small amounts of hydrogen, while not necessary, were found to accelerate the rate. (However, larger amounts of hydrogen had no effect on the reaction and hydrogen is not part of the rate equation.)

$$H_2C{=}CH_2 + CO + ROH \rightarrow CH_3CH_2C(=O)OR,$$
$$R = H\text{–},\ Me\text{–},\ CH_3CH_2C(=O)\text{–} \qquad (1)$$

Whereas this earlier report described the reaction in detail, including the identification of the by-products,

*Corresponding author. Fax: +1-615-229-4558; e-mail: jzoeller@eastman.com

0920-5861/99/$ – see front matter
PII: S0920-5861(98)00457-X

detailed kinetics, and proposed a mechanistic interpretation, space limitations precluded a detailed discussion of the spectroscopic investigation. However, the in situ infrared spectroscopic studies, were important in understanding the behavior of the Mo species under reaction conditions. In this paper, we will describe the in situ infrared spectroscopic investigations used to elucidate the chemistry of the key Mo intermediates under reaction temperature and pressure.

2. Experimental

The infrared spectra were collected using an ASI, Applied System's ReactIR™ 2000, Fourier transform infrared spectrometer system. The system was equipped with a liquid nitrogen cooled MCT detector and interfaced to an Autoclave Engineer's 300 ml Hastelloy C autoclave. The autoclave was specially modified to include a 30° silicon ATR element with a useable operating range from 4000 to 1500 wave numbers. The autoclave and associated control system were capable of operation at pressures up to 102 atm and a maximum operating temperature of 300°C. A diagram of the apparatus appears in Fig. 1.

For a typical investigation, the autoclave was first cleaned by charging 200 ml propionic acid. The autoclave was sealed, pressurized to 13.6 atm with nitrogen and heated to 100°C while stirring at 500 rpm. After 30 min at temperature and

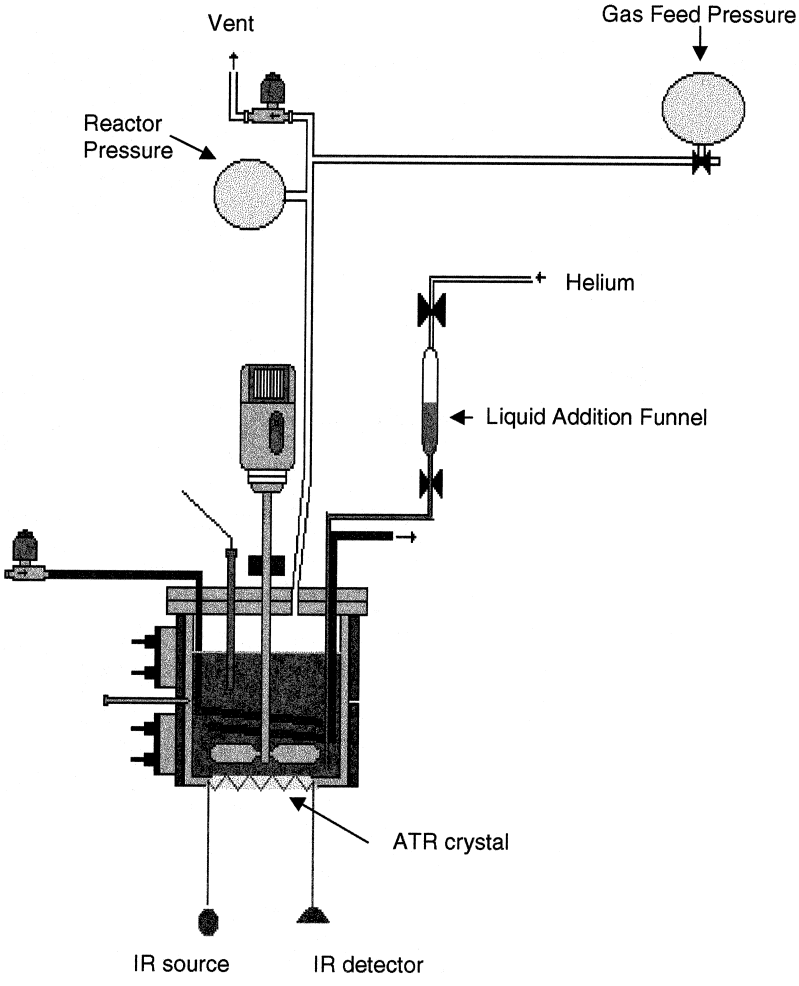

Fig. 1. This figure illustrates the experimental setup and the incorporation of the infrared spectrometer.

pressure, the autoclave contents were cooled to 30°C prior to removal from the autoclave. This treatment was followed in each case by one or more further rinses with propionic acid at ambient temperature.

The reactants were then charged to the autoclave. Solids, e.g., 6.88 g $Mo(CO)_6$ and 22.57 g tetrabutyl phosphonium iodide, were first charged to the clean autoclave, followed by addition of the solvent/reactants, e.g., 200.0 g of propionic acid. (The added solids are completely soluble under the reaction conditions and the recovered solutions are homogeneous.) The autoclave was purged with nitrogen and then with carbon monoxide. The purge process was to bring the system to 13.6 atm pressure while stirring at 500 rpm, turn off the stirrer, vent the pressure. The purge procedure was repeated two times or more for both nitrogen and CO. The vent was then closed, the experimental pressure applied, usually 23–27 atm with CO, the stir rate set to 750 rpm, and heat applied to bring the system to 160°C. In some cases, where the effect of a second component was examined, that material, e.g., 52.0 g ethyl iodide, was added via an auxiliary high pressure addition funnel. To add the contents of the addition funnel, the funnel was placed under a helium atmosphere whose pressure exceeded the equilibrium pressure in the autoclave by 5–10 atm. The contents were then added by simply opening the valve on the high pressure liquid addition funnel.

ASI Applied System's reaction monitoring software V2.1 was employed to collect spectra as a function of time and reaction condition.

3. Results and discussion

Prior to discussing the spectroscopy results, it is useful to review the results of the kinetic investigations and the resultant mechanistic proposal [1]. The mechanistic proposal is presented in Scheme 1, Equation (2–16) [1]. Using the steady state approximation, it follows that the rate equation is given by Eq. (17). (The rate constants (k_i) in Eq. (17) correspond to the reactions in Scheme 1.) The results of the kinetic investigation and a comparison with the rate orders predicted by rate Eq. (17) are summarized in Table 1.

Table 1
Expected and observed reaction orders for the halide promoted carbonylation of ethylene to propionic anhydride

Reaction component	Expected reaction order	Observed reaction order
Ethylene	0	0.06
Carbon monoxide	$(1–1.5)^{-1}$	$(1.17)^{-1}$
Hydrogen	0	Zero after 3 atm
$Mo(CO)_6$	0.5	0.62
Bu_4PI	1	0.99
Ethyl iodide (EtI)	Complex[a]	Complex

[a]Expected rate order for ethyl iodide should fit a general equation

$$\text{Rate} = C_1[\text{EtI}]^{1/2}/(C_2 + [\text{EtI}])^{1/2},$$

if all other variables are held constant. This matches the observed behavior.

$$\text{Rate} = \frac{k_6 k_2^{1/2}[\text{EtI}]^{1/2}[\text{Mo(CO)}_6]^{1/2}[\text{I}^-]}{k_{13}^{1/2}[(k_{-2}/k_3)[P_{\text{CO}}]+[\text{EtI}]]^{1/2}[(k_{-6}/k_7)[P_{\text{CO}}]+1]}. \quad (17)$$

In addition to the kinetic indications, the reaction is significantly inhibited by the free radical scavenger duroquinone and coupling products are observed. Both of these additional observations strengthened the case for a free radical process.

Whereas the kinetics were the most important mechanistic indicators, in situ infrared spectroscopy provided significant insight into several of the reaction steps involving Mo catalyzed ethylene carbonylation.

Generally, these reactions are very fast and unless one deliberately restricts the reaction, the reacting system can quickly become mass transfer limited. The desired slower operating regimes can be achieved by either the application of lower temperatures or since the reaction is inverse order in CO, the application of higher CO pressures. Further, this Mo catalyzed reaction is sufficiently fast that, if all the reaction components are present in the reactor at the outset, the reaction is approaching completion before the autoclave reaches (and equilibrates at) the desired temperature. In the earlier kinetic studies, we avoided this problem by using a purged autoclave and did not introduce the ethylene until we wished to initiate reaction (1).

In the spectroscopic studies, where the catalyst concentrations had to be substantially higher to obtain good spectra, we used a similar, stepwise approach.

Initiation (Catalyst Generation/Activation)

$$Mo(CO)_6 \rightleftharpoons Mo(CO)_5 + CO \quad (2)$$

$$Mo(CO)_5 + EtI \longrightarrow \bullet Mo(CO)_5I + Et\bullet \quad (3)$$

$$\bullet Mo(CO)_5I + EtI \longrightarrow Mo(CO)_5I_2 + Et\bullet \quad (4)$$

$$Mo(CO)_6 + Et\bullet \longrightarrow \bullet Mo(EtCO)(CO)_5 \quad (5)$$

Propagation (Catalytic Process)

$$\bullet Mo(EtCO)(CO)_5 + I^- \rightleftharpoons \bullet Mo(EtCO)(CO)_4I^- + CO \quad (6)$$

$$\bullet Mo(EtCO)(CO)_4I^- \longrightarrow \bullet Mo(CO)_4^- + EtCOI \quad (7)$$

$$\bullet Mo(CO)_4^- + CO \longrightarrow \bullet Mo(CO)_5^- \quad (8)$$

$$\bullet Mo(CO)_5^- + H^+ \longrightarrow \bullet MoH(CO)_5 \quad (9)$$

$$\bullet MoH(CO)_5 + C_2H_4 \longrightarrow \bullet Mo(CO)_5Et \quad (10)$$

$$\bullet Mo(CO)_5Et + CO \longrightarrow \bullet Mo(EtCO)(CO)_5 \quad (11)$$

$$EtCOI + EtCOOH \longrightarrow (EtCO)_2O + HI \text{ (Product Formation)} \quad (12)$$

Termination (Catalyst Deactivation)

$$2 \bullet Mo(EtCO)(CO)_5 \xrightarrow{2\,CO} EtCOCOEt + 2\,Mo(CO)_6 \quad (13)$$

Catalyst Regeneration (Reduction of Mo(II) by hydrogen)

$$Mo(CO)_5I_2 + I^- \longrightarrow Mo(CO)_4I_3^- \text{ (observed)} \quad (14)$$

$$Mo(CO)_4I_3^- + H_2 + CO \longrightarrow 2HI + Mo(CO)_5I^- \quad (15)$$

$$Mo(CO)_6 + I^- \rightleftharpoons Mo(CO)_5I^- + CO \quad (16)$$

Scheme 1. Proposed mechanism for the generation of propionic anhydride from ethylene, CO, and propionic acid

We initially added the $Mo(CO)_6$ and the salt, $[Bu_4P]I$, and propionic acid to the autoclave, sealed the autoclave, and thoroughly purged the autoclave first with nitrogen and then with CO. After thoroughly purging with CO, the autoclave was pressurized to 23.8 atm using carbon monoxide and heated to 160°C. Vapor pressure increased the autoclave pressure to 27.2 atm. Spectra were then recorded.

A strong peak was observed at 1987 cm^{-1} corresponding to $Mo(CO)_6$ and a second, weaker peak, was observed at 1933 cm^{-1} corresponding to $Mo(CO)_5I^-$ [2,3] (see Fig. 2). This observation indicated that, under these reaction conditions, an equilibrium between $Mo(CO)_6$ and $Mo(CO)_5I^-$ (reaction (18)) was observed which favored the hexacarbonyl species.

$$Mo(CO)_6 + I^- \rightleftarrows Mo(CO)_5I^- + CO \quad (18)$$

Ethyl iodide was then added via a liquid addition funnel and spectra were recorded. Upon addition of the ethyl iodide, additional peaks began to arise (see Fig. 3). These peaks are located at 2068 cm^{-1} and as shoulders to the peaks at 1987 and 1933 cm^{-1} centered at 2012 and 1943 cm^{-1}, respectively. Subtraction of the spectrum in Fig. 2, reveals peaks at 2068(s), 2012(vs), 1989(s), and 1943(m) cm^{-1} (see Fig. 4). These peaks correspond well with those reported in the literature for $Mo(CO)_4I_3^-$. (King [4] reports peaks at 2065(s), 2003(s), 1994(s), 1964(s), and 1944(s) cm^{-1} for the methyl pyridinium salt, while

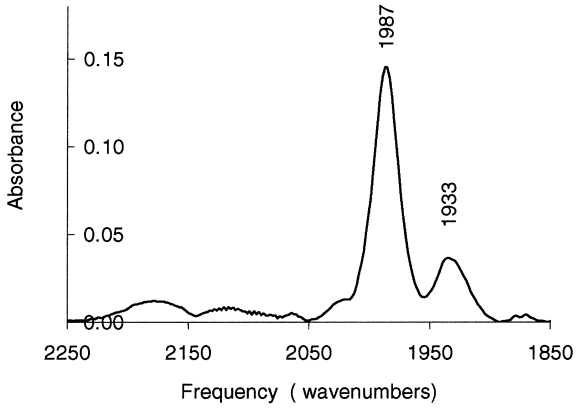

Fig. 2. Infrared spectrum observed for 6.9 g $Mo(CO)_6$+22.5 g Bu_4PI in 200 g propionic acid at 160°C and 27.2 atm CO.

Ganorkar and Stiddard [5] report peaks at 2083(m), 2018(vs), 1961(s) and 1942(s) cm^{-1}.) This reflects a two electron oxidation of the catalyst by ethyl iodide.

The addition of ethylene to the system to begin the reaction did not lead to any additional peaks but did effect the relative ratios of the peaks. We could only obtain a few spectra as these reaction conditions led to very high rates and the reaction rapidly becomes CO depleted leading to catalyst decomposition. We also need to use caution in interpreting the shift in relative ratios of the different components since as CO is

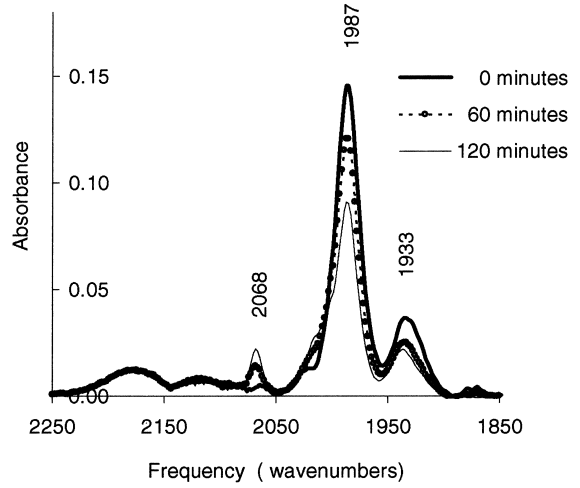

Fig. 3. Change observed on addition of 52 g EtI to 6.9 g $Mo(CO)_6$ and 22.5 g Bu_4PI in 200 g propionic acid at 160°C and 27.2 atm CO.

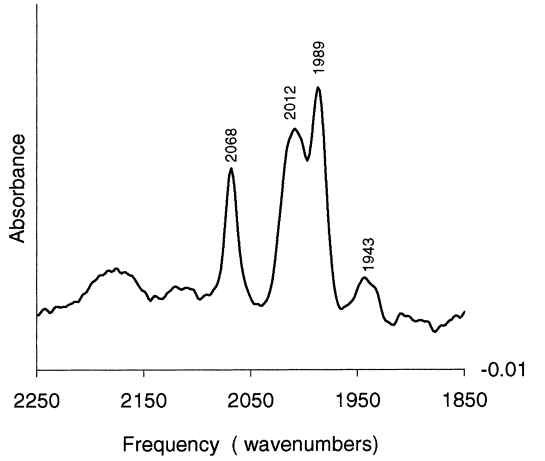

Fig. 4. Residual spectrum generated by subtracting the spectrum of $Mo(CO)_6$ and that of $Mo(CO)_5I^-$ from that observed 60 min after addition of EtI (refer to Fig. 2).

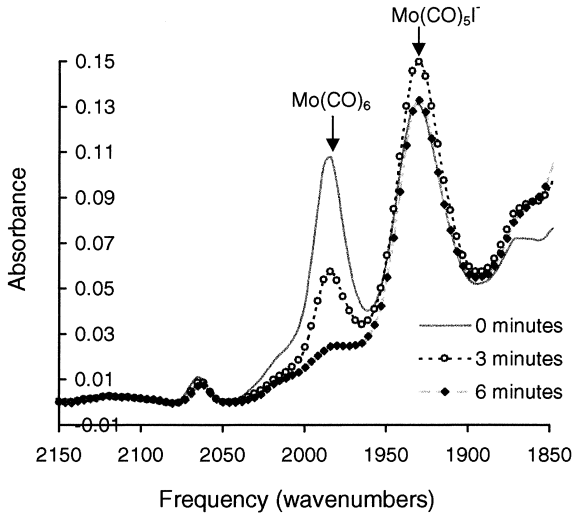

Fig. 5. Spectral changes for metal carbonyl species upon reaction with ethylene/CO over a 6 min time frame.

depleted, it is likely to effect the ratio of the components. Typical behavior is shown in Fig. 5.

While this one simple experiment gave us a substantial amount of information about the catalyst species, we looked at each step in more detail. Reviewing the above experiment, there were several key areas where in situ infrared spectroscopy would further elucidate the behavior of Mo in this catalytic process, namely:

1. Quantifying and elucidating the role of the potentially important equilibrium between $Mo(CO)_6$ and $Mo(CO)_5I^-$ shown in reaction (18).
2. Clarifying the interaction of ethyl iodide with the zero valent Mo species.
3. Clarifying the role of hydrogen.

In addition, the in situ spectroscopy proved to be useful in interpreting the duroquinone inhibition.

We began our studies by obtaining details regarding the equilibrium between $Mo(CO)_6$ and $Mo(CO)_5I^-$ (reaction (18)) since we initially thought this equilibrium was going to be critical in understanding the catalysis. Before we had any kinetic data, we suspected, based on the spectroscopic results, that the initiating steps in this catalysis were the generation of $Mo(CO)_5I^-$ followed by either displacement of the iodide by an S_N2 (or possibly S_N1) reaction, as shown in reaction (19) or protonation of $Mo(CO)_5I^-$ (forming $HMo(CO)_5I$), as shown in reaction (20), which would initiate a hydride based process. Both are familiar starting points for classical catalytic processes for the carbonylation of ethylene and we used these as our initial starting mechanistic hypotheses. Further, even when it became apparent that this reaction was fractional order in Mo, we thought this equilibrium was likely to be significant since pre-equilibria are often responsible for apparent fractional order type behaviors.

$$Mo(CO)_6 + I^- \rightleftarrows Mo(CO)_5I^- + CO \qquad (18)$$

$$Mo(CO)_5I^- + EtI \rightarrow EtMo(CO)_5I + I^- \qquad (19)$$

$$H^+ + Mo(CO)_5I^- \rightarrow HMo(CO)_5I \qquad (20)$$

As the kinetics began to develop, it became apparent that there was a cation effect in which the rates could differ by more than an order of magnitude. We strongly believed that this equilibrium may have been responsible. However, as we will see, this equilibrium, while interesting, was primarily a spectator process and this first mechanistic proposal would be proven invalid in the light of the combined kinetics and spectroscopic evidence.

Our first efforts were devoted to establishing the equilibrium constant for the reaction in propionic acid so that we could directly determine the concentrations of each Mo species and ultimately the concentration of the iodide anion as well. These measurements were not trivial since the spectral observations are carried out above the normal boiling point of the reaction medium and under elevated pressure. Therefore the requisite indices of refraction needed to calculate the effective path length (l) were not available nor were we likely to get access to these numbers. Further, although they might be determined with considerable difficulty and expense using alternative methods, we did not have access to good estimates of the extinction coefficients (ϵ) for either species in this reaction media at these operating temperatures.

Despite the inability to readily access either the effective path length (l) or an accurate estimate of the extinction coefficient (ϵ) for each species directly, we found that we could determine the equilibrium constant in the absence of this information by varying the pressure of a single sample of $Mo(CO)_6$ and an iodide salt, in this case tetrabutyl phosphonium iodide, at a fixed temperature. (A temperature effect on the equilibrium could also be conducted with a fixed pressure.) To accomplish this, we recorded the absorbances of $Mo(CO)_6$ at 1986 cm^{-1} and $Mo(CO)_5I^-$ at 1935 cm^{-1} at equilibrium over a number of pressures. (Experimentally, the system was regarded as at equilibrium when no further change occurred in the spectrum over time.) The absorbance for each species as a function of pressure is shown in Fig. 6.

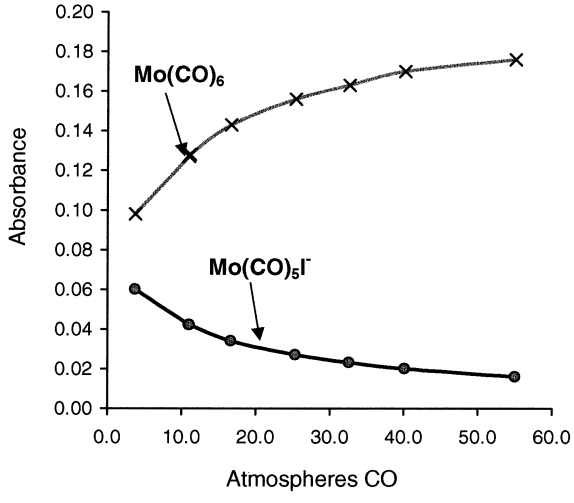

Fig. 6. Spectral dependence upon CO pressure for the major species $Mo(CO)_6$ and $Mo(CO)_5I^-$ measured at 160°C; (6.9 g $Mo(CO)_6$, 22.5 g Bu_4PI, and 200 g propionic acid).

Since there are only two carbonyl species observed under these conditions

$$\mathrm{Mo_0}= \text{added } \mathrm{Mo(CO)_6}/\text{vol} = [\mathrm{Mo(CO)_5I^-}] + [\mathrm{Mo(CO)_6}] = \text{total } [\mathrm{Mo}]. \quad (21)$$

Assuming Beer's law holds

$$[\mathrm{Mo(CO)_6}] = A_{\mathrm{Mo(CO)_6}}/\epsilon_{\mathrm{Mo(CO)_6}} l_{\mathrm{Mo(CO)_6}} \quad (22)$$

and

$$[\mathrm{Mo(CO)_5I^-}] = A_{\mathrm{Mo(CO)_5I^-}}/\epsilon_{\mathrm{Mo(CO)_5I^-}} l_{\mathrm{Mo(CO)_5I^-}}. \quad (23)$$

Therefore,

$$\mathrm{Mo_0} = (A_{\mathrm{Mo(CO)_6}}/\epsilon_{\mathrm{Mo(CO)_6}} l_{\mathrm{Mo(CO)_6}}) + (A_{\mathrm{Mo(CO)_5I^-}}/\epsilon_{\mathrm{Mo(CO)_5I^-}} l_{\mathrm{Mo(CO)_5I^-}}). \quad (24)$$

This can be rearranged to

$$(\mathrm{Mo_0} - A_{\mathrm{Mo(CO)_6}}/\epsilon_{\mathrm{Mo(CO)_6}} l_{\mathrm{Mo(CO)_6}}) \times (\epsilon_{\mathrm{Mo(CO)_5I^-}} l_{\mathrm{Mo(CO)_5I^-}}) = A_{\mathrm{Mo(CO)_5I^-}}, \quad (25)$$

which fits the form of a straight line ($y=mx+b$), wherein $A_{\mathrm{Mo(CO)_6}}$ is the abscissa and $A_{\mathrm{Mo(CO)_5I^-}}$ is the ordinate, and the slope, m, is represented by

$$m = -\left(\epsilon_{\mathrm{Mo(CO)_5I^-}} l_{\mathrm{Mo(CO)_5I^-}}/\epsilon_{\mathrm{Mo(CO)_6}} l_{\mathrm{Mo(CO)_6}}\right). \quad (26)$$

This slope represents the critical relationship needed to determine the relative concentrations of the two components. (Note: Although the intercept, b, should allow us to determine $\epsilon_{\mathrm{Mo(CO)_5I^-}} l_{\mathrm{Mo(CO)_5I^-}}$ directly (intercept $= \mathrm{Mo_0}\epsilon_{\mathrm{Mo(CO)_5I^-}} l_{\mathrm{Mo(CO)_5I^-}}$) these extrapolated numbers tend to be inaccurate and the equilibrium constant and concentrations are determined more directly as shown below.) The plot of $A_{\mathrm{Mo(CO)_6}}$ vs. $A_{\mathrm{Mo(CO)_5I^-}}$ is shown in Fig. 7 (least squares fit data for the plot in Fig. 5: slope=(−0.562), intercept=0.115, R^2=99.9).

The equilibrium constant for reaction (18) can be expressed as

$$K = \frac{[\mathrm{Mo(CO)_5I^-}][P_{\mathrm{CO}}]}{[\mathrm{Mo(CO)_6}][\mathrm{I^-}]} \quad (27)$$

and we can calculate the concentration of each species as follows:

Since

$$\mathrm{Mo_0} = [\mathrm{Mo(CO)_5I^-}] + [\mathrm{Mo(CO)_6}]. \quad (21)$$

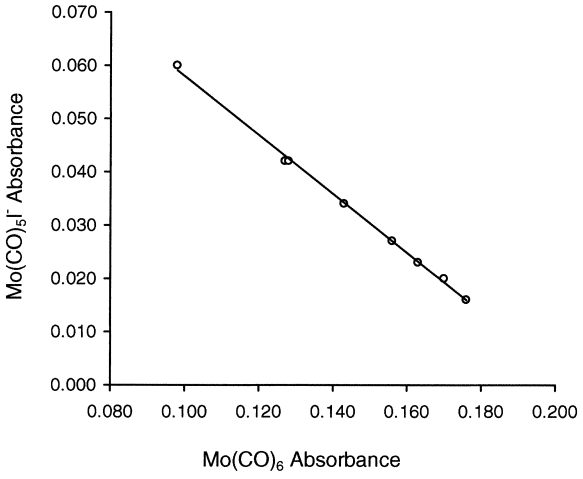

Fig. 7. Plot showing the relationship between $\mathrm{Mo(CO)_6}$ and $\mathrm{Mo(CO)_5I^-}$ as used to determine the relative extinction coefficients.

Then,

$$\frac{[\mathrm{Mo(CO)_6}]}{[\mathrm{Mo(CO)_5I^-}]} = \frac{\mathrm{Mo_0} - [\mathrm{Mo(CO)_5I^-}]}{[\mathrm{Mo(CO)_5I^-}]} = (\mathrm{Mo_0}/[\mathrm{Mo(CO)_5I^-}]) - 1, \quad (28)$$

but

$$\frac{[\mathrm{Mo(CO)_6}]}{[\mathrm{Mo(CO)_5I^-}]} = \frac{A_{\mathrm{Mo(CO)_6}}/\epsilon_{\mathrm{Mo(CO)_6}} l_{\mathrm{Mo(CO)_6}}}{A_{\mathrm{Mo(CO)_5I^-}}/\epsilon_{\mathrm{Mo(CO)_5I^-}} l_{\mathrm{Mo(CO)_5I^-}}} = -m(A_{\mathrm{Mo(CO)_6}}/A_{\mathrm{Mo(CO)_5I^-}}), \quad (29)$$

where m is the slope determined from the plot in Fig. 5.

Therefore,

$$(\mathrm{Mo_0}/[\mathrm{Mo(CO)_5I^-}]) - 1 = -m(A_{\mathrm{Mo(CO)_6}}/A_{\mathrm{Mo(CO)_5I^-}}), \quad (30)$$

this can be rearranged as follows:

$$[\mathrm{Mo(CO)_5I^-}] = \mathrm{Mo_0}/[[(-m)(A_{\mathrm{Mo(CO)_6}}/A_{\mathrm{Mo(CO)_5I^-}})] + 1]. \quad (31)$$

Having $[\mathrm{Mo(CO)_5I^-}]$, $[\mathrm{Mo(CO)_6}]$ is trivial since

$$[\mathrm{Mo(CO)_6}] = \mathrm{Mo_0} - [\mathrm{Mo(CO)_5I^-}]. \quad (32)$$

Before calculating the equilibrium constant, one needs to go back and calculate the iodide salt concentration, $[\mathrm{I^-}]$, as well since some of the iodide is consumed in

forming $Mo(CO)_5I^-$:

I_0= initial concentration of iodide salt

$$= [Mo(CO)_5I^-] + [I^-]. \quad (33)$$

Therefore

$$[I^-] = I_0 - [Mo(CO)_5I^-]. \quad (34)$$

The equilibrium constant is now obtainable for each pressure used in the course of the experiment by simply substituting the values into Eq. (27).

The equilibrium constant was found to be about 39 atm L/mol with a standard deviation of 1 after correction for the vapor pressure of propionic acid. (The equilibrium constant *estimated* in our earlier report was reported as being about 12. This estimate was determined prior to this more rigorous treatment and was incorrect by a factor of 3. However, this underestimation is insufficient to cause any change in the mechanistic interpretation.) We could now calculate the concentration of the two zero valent species in any of our reactions. For example, under our normal reaction conditions from the earlier kinetic study (0.06 M $[Bu_4P]I$, 0.033 M Mo, 23.8 atm CO, 160°C), the concentrations of $Mo(CO)_6$ and $Mo(CO)_5I^-$ are 0.03 and 0.003 M, respectively, when the system is at equilibrium.

We were also able to determine the temperature dependence of this equilibrium constant by varying the temperature over a 40°C range. From the plot of $1/T$ vs. ln K (shown in Fig. 8), the reaction was found to have a ΔH=+3.4 kcal/mol and ΔS=+4.5 cal/mol K.

While conducting this equilibrium study, our kinetic investigations revealed that there was a significant cation effect upon the reaction rate [1]. We sought to resolve the role of the $Mo(CO)_5I^-$ anion and the salt effect by examining the effect several salts had upon equilibrium (18) and correlating these to the reaction rates.

The rate for carbonylation of ethylene to propionic anhydride could vary over an order of magnitude depending on the counterion for the iodide. However, in most of the extreme cases low rates might be assignable to other factors, such as solubility, or steric hindrance may have inhibited an in situ quarternization, so we focused on three of the mid-range processes and attempted to obtain similar determinations of the equilibrium constant. The three salts we focused

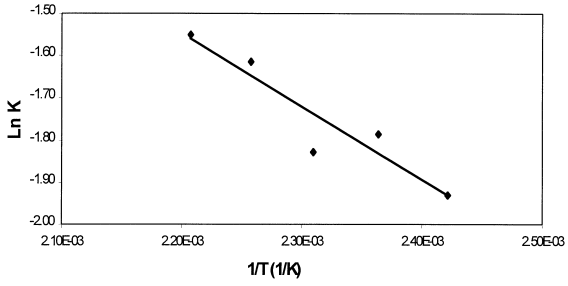

Fig. 8. Plot of ln K vs. $1/T$ for the determination of thermodynamic parameters.

on were pyridinium hydroiodide ([pyH]I), tetrabutyl phosphonium iodide ($[Bu_4P]I$) and NaI which displayed relative reaction rates of 2.8:1.8:1, respectively, for the carbonylation of ethylene to propionic anhydride. (In our kinetic runs, NMR revealed that pyridine is converted to pyridinium hydroiodide. The HI was generated in situ by elimination from ethyl iodide. Little or no alkylation of the pyridine was observed.)

We attempted to determine the equilibrium constants for each of these salts using the techniques and information obtained from the $[Bu_4P]I$. Whereas the equilibrium constant using [pyH]I was readily attainable and found to be 21(±3) atm L/mol, we were unable to get an equilibrium constant for NaI because *there was no significant amount of* $Mo(CO)_5I^-$ *formed* (see Fig. 9).

These results indicate that there is no correlation between the concentration of $Mo(CO)_5I^-$ to the rate of the reaction. Whereas, in the case of NaI, the quantity of $Mo(CO)_5I^-$ present is below detection limits, the reaction still runs, albeit at only about 55% of the rate using $[Bu_4P]I$. Further, when using [pyH]I, the concentration of $Mo(CO)_5I^-$ can be calculated under standard reaction conditions (0.06 M [pyH]I, 0.033 M Mo, 23.8 atm CO, 160°C), and is found to be about 1.5×10^{-3} M or half that using $[Bu_4P]I$. Despite the concentration of $Mo(CO)_5I^-$ being halved, the reaction rate using [pyH]I is nearly 55% faster than when $[Bu_4P]I$ was used as the salt.

This portion of the study played a key role in directing us away from our first hypothesis and was one of the several observations which forced us to seek an alternative mechanism to explain the first order behavior of iodide and fractional order behavior of

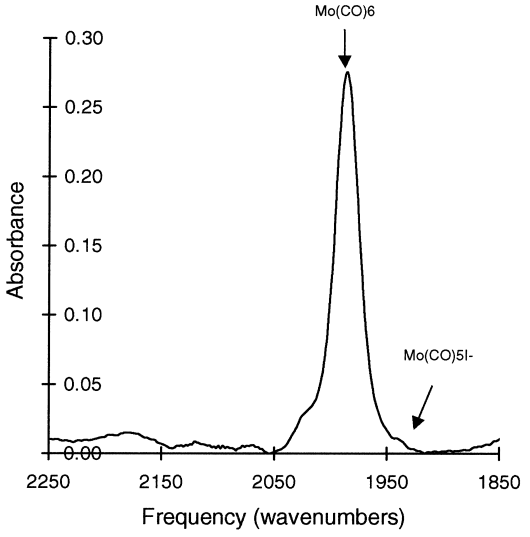

Fig. 9. The relative concentration of $Mo(CO)_6$ to $Mo(CO)_5I^-$ for the reaction of 6.9 g $Mo(CO)_6$+17.5 g NaI in 200 g propionic acid at 160°C and 27.2 atm CO.

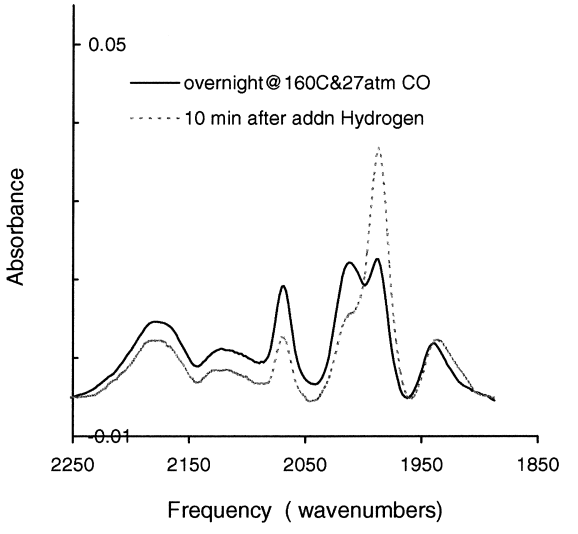

Fig. 10. Effect of adding hydrogen (23.8 atm) to a solution of $Bu_4PI/Mo(CO)_6$ which had been oxidized by EtI.

Mo. As we now understand equilibrium (18), it is apparently a spectator process. Further, $Mo(CO)_5I^-$ is a higher energy species (by >3 kcal/mol) than $Mo(CO)_6$. As such, it is likely to dissociate an iodide to form the key intermediate, $Mo(CO)_5$, which initiates catalysis (see Scheme 1), even faster than $Mo(CO)_6$ dissociates CO.

With an understanding of this equilibrium completed, we turned our attention to the interaction of ethyl iodide with the equilibrium mixture of $Mo(CO)_6$ and $Mo(CO)_5I^-$. We already described the observations made upon the addition of ethyl iodide to this mixture (see Figs. 2 and 3 along with the accompanying text above). Reiterating, the addition of ethyl iodide to the mixture of the zero valent Mo species partially oxidizes the mixture to $Mo(CO)_4I_3^-$. A similar oxidation has been observed when $(dmpe)_2Mo(CO)_2$ (dmpe=1,2-(dimethylphosphino)ethane) was treated with benzyl bromide [6,7] wherein $[(dmpe)_2Mo(CO)_2Br]Br$ is formed along with 1,2-diphenylethane via a sequence of two outer sphere electron transfer processes. In our mechanistic proposal, we also proposed a one electron transfer process, but believed that, for reaction (3) in our proposal, an inner sphere process was more likely to be operative. We based this belief on the lack of a significant halide effect (indicating electron transfer) and the activation parameters which indicated that the rate limiting step was a dissociation of CO from $Mo(CO)_6$ indicative of an inner sphere process. (Since the earlier report, we have obtained additional evidence supporting our conclusions regarding the nature of the fundamental interaction of EtI with the zero valent Mo species. Addition of a polar aprotic solvent markedly accelerates the reaction [8] as is consistent with an electron transfer process [9,10].)

The oxidation $Mo(CO)_6$ and $Mo(CO)_5I^-$ to $Mo(CO)_4I_3^-$ by ethyl iodide can be partially reversed by the addition of hydrogen. This is demonstrated in Fig. 10 in which one can clearly see that the peaks at 2068 and 2102 cm^{-1} assignable to $Mo(CO)_4I_3^-$ are reduced. The reduction in the peaks assignable to $Mo(CO)_4I_3^-$ are accompanied by an increase in the 1987 cm^{-1} peak assignable to $Mo(CO)_6$. We have interpreted this hydrogen addition to indicate that the role of hydrogen is to return the Mo, which was oxidized by ethyl iodide, to the zero valent state where it is again available for initiating the catalytic process.

It is worth noting that, in an enclosed system, we cannot completely oxidize the Mo to $Mo(CO)_4I_3^-$ with ethyl iodide nor could we completely eradicate $Mo(CO)_4I_3^-$ with hydrogen under these conditions. During our kinetic experiments, we noticed that, if hydrogen was omitted, it was spontaneously generated

anyway. (This was accompanied by a steady decrease in activity as the hydrogen was steadily purged from our reactor.) This would imply that there is not only an equilibrium between the two Mo(0) species but also between $Mo(CO)_4I_3^-$ and the Mo(0) species as shown in Eq. (35) and all three species are present in a steady state concentration under the conditions used to study the reaction by in situ infrared spectroscopy.

$$Mo(CO)_6 + I^- \underset{+CO}{\overset{-CO}{\rightleftarrows}} Mo(CO)_5I^- \underset{+H_2,-2HI}{\overset{(2EtI,-2Et\cdot)\ \text{or}\ 2HI,-H_2}{\rightleftarrows}} Mo(CO)_4I_3^- + CO \quad (35)$$

However, although this equilibrium is likely to be operative in the absence of ethylene (as in our in situ spectroscopic study of the reaction), in the catalytic carbonylation of ethylene, HI is continuously consumed by the equilibration of ethylene and HI with ethyl iodide as shown in Eq. (36). In the presence of ethylene, which continuously consumes HI, the equilibrium is shifted toward the zero valent Mo species and, under catalytic conditions where sufficient hydrogen is also supplied, the steady state concentration of divalent $Mo(CO)_4I_3^-$ is likely to be quite small.

$$HI + H_2C = CH_2 \rightleftarrows EtI \quad (36)$$

There was one last contribution made by the in situ infrared spectroscopic studies. One key experiment we undertook in our kinetic studies was the suppression of the reaction rate by duroquinone. We were quite concerned that duroquinone might be an adequate oxidant for $Mo(CO)_6$ and $Mo(CO)_5I^-$. However, when duroquinone is added to an equilibrium mixture of $Mo(CO)_6$ and $Mo(CO)_5I^-$ under pressure, the spectroscopy showed no observable oxidation of the Mo species. Thus indicating that the inhibition by duroquinone is assignable to its normal role as a trap for free radicals, not as an oxidant which deactivates Mo(0) by converting it to Mo(2+) species.

4. Conclusion

From the in situ infrared experiments, it was clear that the identifiable Mo species present during the course of the iodide promoted carbonylation of ethylene with Mo catalysts are $Mo(CO)_6$, $Mo(CO)_5I^-$, and $Mo(CO)_4I_3^-$. The zero valent species, $Mo(CO)_6$ and $Mo(CO)_5I^-$, are in equilibrium with one another, with $Mo(CO)_6$ being the favored species under catalytic reaction conditions. We have quantified this equilibrium, but find that there is no correlation between the equilibrium constant and the reaction rates for the carbonylation of ethylene implying the iodide effect arises somewhere else in the mechanism.

Using in situ infrared spectroscopy, we have also demonstrated that the zero valent species are oxidized to $Mo(CO)_4I_3^-$ by the addition of ethyl iodide. This is consistent with historical precedent and our proposed mechanism.

This oxidation could be reversed with hydrogen. In the catalytic carbonylation of ethylene, hydrogen apparently serves to regenerate the catalyst by reducing the oxidized $Mo(CO)_4I_3^-$ to zero valent species.

Acknowledgements

We wish to thank the US Department of Energy and Eastman Chemical Company for their joint support of this work under US Department of Energy Contract no. DE-AC22-94PC94065.

References

[1] J.R. Zoeller, E.M. Blakely, R.M. Moncier, T. Dickson, Catal. Today 36 (1997) 227.
[2] E.W. Abel, I.S. Butler, J.G. Reid, J. Chem. Soc. (1963) 2068.
[3] E.W. Abel, I.S. Butler, G. Wilkenson, Chem. Ind. (1960) 442.
[4] R.B. King, Inorg. Chem. 3 (1964) 1039.
[5] M.C. Ganorkar, M.H.B. Stiddard, J. Chem. Soc. (1965) 3494.
[6] J.A. Conner, P.I. Riley, J. Chem. Soc., Dalton Trans. (1979) 1318.
[7] J.A. Conner, P.I. Riley, J. Chem. Soc., Chem. Commun. (1976) 634.
[8] J.R. Zoeller, US Patent 5 760 284 (1998).
[9] T.A. Huber, D.H. Maccartney, M.C. Baird, Organometallics 14 (1995) 592.
[10] J.P. Collman, L.S. Hegedus, J.R. Norton, R.G. Finke, Principles and Applications of Organotransition Metal Chemistry, Chapter 5, University Science Books, Mill Valley, CA, 1987.